

# Simulation of Heat Transfer on Periodic Microstructured Surfaces for Evaporation Cooling

Matthias Hackert-Oschätzchen<sup>\*1</sup>, Raphael Paul<sup>1</sup>, Michael Penzel<sup>1</sup>, Mike Zinecker<sup>1</sup>, Andreas Schubert<sup>1,2</sup>

<sup>1</sup>Technische Universität Chemnitz, Professorship Micromanufacturing Technology, Germany

<sup>2</sup>Fraunhofer Institute for Machine Tools and Forming Technology IWU, Chemnitz, Germany

\*09107 Chemnitz, Germany, matthias.hackert@mb.tu-chemnitz.de

**Abstract:** Evaporative cooling is a promising cooling method for dissipating high heat fluxes in high power density applications [1,2]. One possibility to enhance heat flux is a generation of microstructures into the cooler surface. This enlarges the cooler surface and systematically affects the fluid flow as well as the boiling process [1]. In this study the geometric arrangement of cylindrical pin microstructures with small aspect ratio was investigated by analyzing the conductive and convective components of heat transfer. Using COMSOL Multiphysics a 3D model with the non-isothermal flow interface was created.

**Keywords:** Evaporative Cooling, Micro-Structured Surface, Non-isothermal Flow

## 1. Introduction

The growing power density of electronic devices requires the development of new cooling methods and systems by which large heat fluxes can be dissipated. In this respect evaporative cooling is an innovative and promising method. [1,2] In addition to convective heat dissipation like in usual water cooling systems the boiling fluid absorbs vaporization heat. Beside the operating mode “natural circulation”, which is driven by natural convection, there is the operating mode “forced circulation”. In this case the fluid flow is generated by applying an external pressure difference, that enables high flow velocities. Thus emerging vapor bubbles are removed quickly from the cooler surface and a high convective cooling performance can be achieved.

In order to enhance heat transfer microstructures are machined into the cooler surface. That enlarges the heat transfer coefficient by enlarging the cooler surface and manipulating the fluid flow as well as the boiling process. [1]

For preselecting promising microstructures for experiments and for understanding

differences in thermodynamic performance a COMSOL Multiphysics model was built up. The model analyzes the conductive and convective components of heat transfer. In this study the model is applied to investigate the influence of the geometrical arrangement of pins at three different inflow velocities.

## 2. Model design

Figure 1 shows the top view and a 3D view on the two analyzed microstructures.

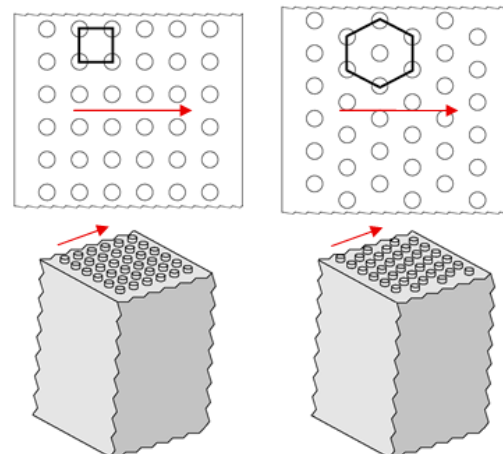


**Figure 1.** Analyzed microstructures, left: cubic pin arrangement; right: hexagonal pin arrangement

The arrows betoken the inflow direction. In the left microstructure the arrangement is cubic; in the right one it is hexagonal. The pin diameter is 100  $\mu\text{m}$  and the pin height is 50  $\mu\text{m}$ . The horizontal and vertical center distance between the pins amounts 200  $\mu\text{m}$ . In the hexagonal arrangement every second pin row is vertically displaced by half the center distance. As cognizable in Figure 1 both structures feature symmetry planes. The flow condition is considered to be stable and symmetric at any time and inflow velocity. Thus it is not necessary to implement the whole geometry. Based on that assumption a periodic 3D model with non-

isothermal flow was created. The equations for conservation of mass, momentum and energy were solved without turbulence model in a stationary study.

Figure 2 shows the implemented model geometry.

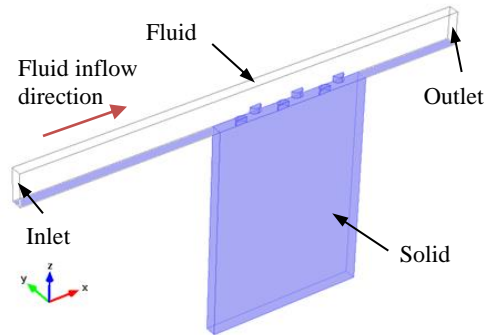


**Figure 2.** Implemented model geometry showcase for hexagonal pin arrangement

The colored domain represents a cutaway of the cooler. The boundary conditions for the walls of the undersurfaces of the fluid domain are defined as no-slip. The inlet condition is normal inflow velocity where  $U_0$  varies between  $U_{0a} = 2$  m/s,  $U_{0b} = 5$  m/s and  $U_{0c} = 7$  m/s. The outlet condition is pressure, no viscous stress. The remaining top and side faces of the fluid domain were defined as slip walls. As thermodynamic boundary conditions the undersurface of the solid body was set to  $70^\circ\text{C}$  and the inlet boundary to  $20^\circ\text{C}$ . Thermal insulation was defined for the remaining outer surfaces except the outlet boundary. There the outflow boundary condition was defined.

### 3. Meshing

Figure 3 shows the created mesh with the finest parameter settings. Additionally to the geometry in Figure 2 a mesh refining domain with twice the structure height was defined on top of the solid domain. The mesh refining domain is blue colored in Figure 3. On the no-slip condition boundaries a boundary layer mesh with five layers was generated. For a mesh convergence study the mesh was built up parametrically. With the finest parameter settings the complete mesh consists of 4.047 million mesh elements in the cubic pin arrangement.

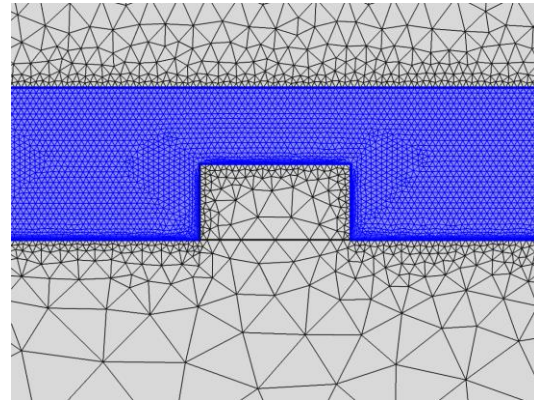


**Figure 3.** Mesh near the first pin, finest parameter settings, hexagonal pin arrangement

## 4. Results

### 4.1 Fluid dynamics

Figure 4 and Figure 5 show streamlines in the velocity field for both cubic and hexagonal pin arrangement at  $U_0 = U_{0a} = 2$  m/s.

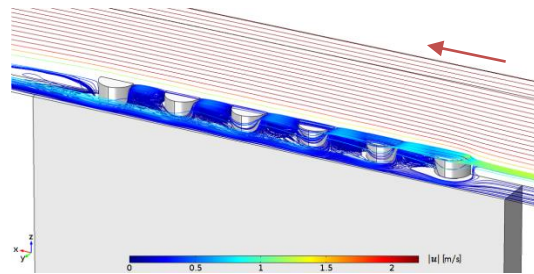


**Figure 4.** Streamlines velocity field cubic pin arrangement  $U_0 = U_{0a} = 2$  m/s

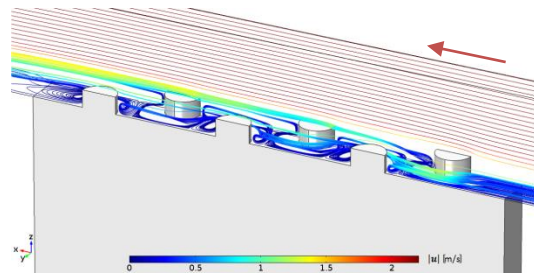


**Figure 5.** Streamlines velocity field hexagonal pin arrangement  $U_0 = U_{0a} = 2$  m/s

The streamline color displays the velocity norm and the arrows betoken the main flow direction. In both figures the same streamline starting points were used. In the upper regions of the fluid domain streamlines are almost parallel in both cases. Following the negative  $z$ -direction

50  $\mu\text{m}$  above the pin tops, the structures influence becomes increasingly intense and significant differences between cubic and hexagonal pin arrangement appear.

In the cubic pin arrangement the influence above the pin tops remains low. Behind the pins cyclic flows develop. These transport fluid from the pin tops to the structure bottom and into the structure deepening which lies between the pins and in line with the  $x$ -direction. There the fluid flows nearly parallel to the main flow direction over the remaining structure length near the solid body surface.

In the hexagonal pin arrangement the influence above the pin tops is much higher. Starting from the second pin row fluid from the lowest fluid layers streams towards a pins front and gets redirected into  $y$ -direction. Then it hits the pins rear side which is situated diagonally in front of the former pin. Thereby it gets redirected into  $z$ -direction and over the pin tops out of the structure. This flow profile can implicate an advantage for evaporative cooling since emerged bubbles are removed quickly from the solid body surface what prevents film boiling.

The differences in fluid dynamics can be summarized as following:

- Cubic pin arrangement: fluid flows from the pin tops to the structure bottom
- Hexagonal pin arrangement: fluid flows from the lowest fluid layers up over the pin tops.
- In the hexagonal pin arrangement the influence ranges higher over the structure tops.
- In the hexagonal pin arrangement a stronger fluid stirring occurs.
- In the hexagonal pin arrangement fluid reaches higher velocities after that it was close to the solid body surface.

## 4.2 Thermodynamics

For describing structural differences in thermodynamics the results at  $U_0 = U_{0c} = 7 \text{ m/s}$  are regarded. Figure 6 and Figure 7 show streamlines in the total heat flux density field. In both figures the streamlines have the same starting points at the undersurface of the solid body.

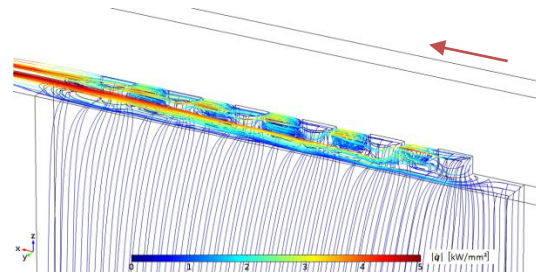


**Figure 6.** Streamlines heat flux density field cubic pin arrangement  $U_0 = U_{0c} = 7 \text{ m/s}$

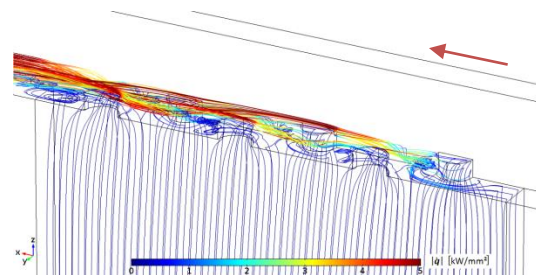


**Figure 7.** Streamlines heat flux density field hexagonal pin arrangement  $U_0 = U_{0c} = 7 \text{ m/s}$

In the cubic pin arrangement in Figure 6 the heat flux streamlines go nearly parallel up from the bottom of the solid body. As they come closer to the solid body top they begin to bend towards the fluid inflow and concentrate in the pins. After that they have exited the solid body, convection becomes the determining part of heat flux and the total heat flux density norm rises. Heat flux streamlines which exited the solid body at the pin tops follow the mentioned cyclic flows and run into the structure deepening which is in line with the  $x$ -direction.

In the hexagonal pin arrangement in Figure 7 the heat flux streamlines go nearly parallel up from the bottom of the solid body, too. They also begin to bend towards the fluid inflow when they come closer to the solid body top and concentrate in the pins. After that they exited the solid body through the pins or the structure bottom they follow the fluid flow. Thus they reach much higher distances to the solid body than in the cubic pin arrangement.

The temperature distributions in the two structure arrangements are shown in Figure 8. Additionally the figure shows the results for a reference cooler with plane surface. The arrow betokens the main flow direction.

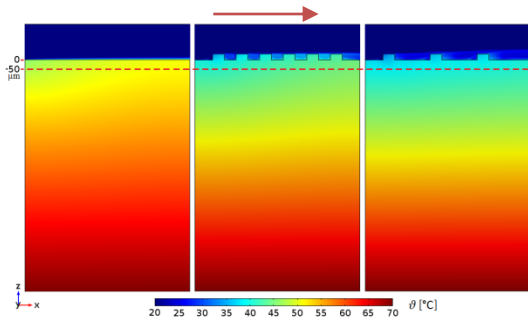


**Figure 8.** Temperature distribution  $U_0 = U_{0c} = 7$  m/s, left: plane surface; middle: cubic pin arrangement; right: hexagonal pin arrangement

In the reference cooler type with plane surface the temperature drops very slowly with the positive  $z$ -direction. In the solid body the lowest temperatures occur near the fluid inlet. The average temperature in the solid body at  $50 \mu\text{m}$  below the surface amounts  $49.6^\circ\text{C}$ . Only a very thin fluid layer close to the solid body gets heated.

In the cubic pin arrangement the temperature drops visibly faster with the positive  $z$ -direction. Here the lowest solid body temperatures occur in the boundary area of the first pin. The average temperature in the solid body at  $50 \mu\text{m}$  below the surface amounts  $42.6^\circ\text{C}$ . Afar from the solid body surface the fluid reaches much higher temperatures than in the unstructured cooler type. The cyclic flows can be recognized in the temperature field.

In the hexagonal pin arrangement the rapidest temperature drop with the positive  $z$ -direction takes place. In the solid body the lowest temperatures occur in the boundary area of the first pin, too. The average temperature in the solid body at  $50 \mu\text{m}$  below the surface amounts  $39.2^\circ\text{C}$ . Afar from the solid body surface the fluid doesn't reach higher temperatures than in the cubic pin arrangement but a bigger fluid volume gets heated.

Figure 9 shows the results for the overall heat flux. The calculation of the overall heat flux was done by help of a Richardson extrapolation.

In all cooler surface types the overall heat flux rises with increasing inflow velocity. In the investigated velocity range related to the plane cooler surface the cubic pin arrangement enhances heat flux by maximum 30%, the hexagonal pin arrangement even by maximum 50%. The thermo dynamical advantage of microstructures rises with the inlet velocity.

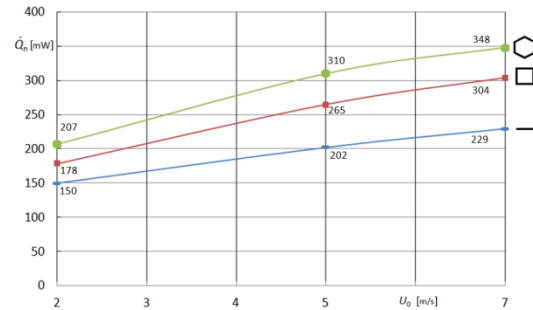


**Figure 9.** Overall heat flux as function of the inflow velocity for all investigated cooler surface types

### 4.3 Heat transfer coefficient

In order to achieve a comparability of results the heat transfer coefficient was calculated by using the following equation: [3]

$$\bar{\alpha} = \left( \frac{A \cdot \Delta T}{\dot{Q}} - \frac{s}{\lambda} \right)^{-1} = \left( \frac{0.14 \text{ mm}^2 \cdot 50 \text{ K}}{\dot{Q}} - \frac{1950 \mu\text{m}}{160 \text{ W}/(\text{m} \cdot \text{K})} \right)^{-1}$$

Therein  $\bar{\alpha}$  is the heat transfer coefficient,  $A$  is the projected area of the cooler surface and  $\Delta T$  is the temperature difference between solid body undersurface and fluid inlet. The distance between solid body undersurface and solid body top (structure bottom) is given by  $s$ . The heat conductivity of the aluminum solid body is  $\lambda$ . For  $\dot{Q}$  the calculated overall heat fluxes were inserted.

Figure 10 shows the calculated heat flux coefficients for all investigated cooler surface types as function of the inflow velocity.

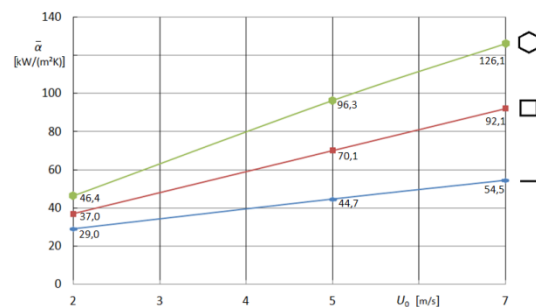


**Figure 10.** Heat flux coefficient as function of the inflow velocity for all investigated cooler surface types



At  $U_0 = U_{0c} = 7$  m/s the cubic pin arrangement enhances the heat flux coefficient by 70% related to the plane cooler surface. With the hexagonal pin arrangement a heightening of 130% is achieved.

The result for the heat transfer coefficient of the plane cooler surface was validated by an analytical calculation according to VDI-Wärmeatlas. [3] The numerically determined values differ less than 2% from the analytically determined values.

## 5. Conclusions

Regarding conductive and convective heat transfer the investigated microstructures with cubic and hexagonal pin arrangement lead to an enhancement of heat transfer. Related to a plane cooler surface the heat transfer coefficient could be enhanced up to maximum 170% with the cubic pin arrangement and up to 230% with the hexagonal pin arrangement. The thermo dynamic advantage of micro-structured cooler surfaces rises with the inflow velocity. The microstructure with hexagonal pin arrangement induces a flow profile which can remove emerged bubbles quickly from the solid body surface. Thereby film boiling can be prevented what is an advantage for evaporative cooling.

## Acknowledgements

This project is funded by the Federal Ministry of Economics and Technology, following a decision of the German Bundestag.

## References

- [1] Schubert, A.; Hackert-Oschätzchen, M.; Meichsner, G.; Zinecker, M.: Design and realization of micro structured surfaces for thermodynamic applications. In: *Microsystem Technologies*, Volume 17, Issue 9, 2011, Pages 1471-1479
- [2] Schubert, A.; Zinecker, M.; Hackert-Oschätzchen, M.; Lausberg, M.; Schulz, A.: Energy-efficient cooling using microstructures for nucleate boiling. In: *Proceedings of the PCIM EUROPE*, 2013, S. 1036-1041, ISBN 978-3-8007-3505-1

- [3] VDI, VDI Wärmeatlas, Gd1-Gd5. Springer-Verlag, Berlin Heidelberg, 2006